ISSN 0838-1992

R. Perla and J. Banner

Hydrology Division
National Hydrology Research Institute
Environment Canada
Saskatoon, Saskatchewan
S7N 3H5

CALIBRATION OF CAPACITIVE CELLS FOR MEASURING WATER IN SNOW

Cold Regions Science and Technology
15(3), October, 225-231, 1988

NHRI Contribution No.88033

1988

90-06486/

3, Oct.

Cold Regions Science and Technology, 15 (1988) 225–231
Elsevier Science Publishers B.V., Amsterdam — Printed in The Netherlands

CALIBRATION OF CAPACITIVE CELLS FOR MEASURING WATER IN SNOW

R. Perla and J. Banner
National Hydrology Research Institute Saskatoon, Saskatchewan (Canada)

(Received February 16, 1988; accepted in revised form April 1, 1988)

ABSTRACT

A capacitive cell is a practical device for measuring liquid water in snow. We have studied the statistical and physical calibration of a one MHz cell using 251 samples, with liquid water measured independently by acid dilution. The assumption that capacitance is a linear function of snow density and liquid water results in an unacceptable model. A nonlinear model with high goodness-of-fit to our data is derived from physical assumptions.

INTRODUCTION

Snow is a mixture of air, ice, liquid water and impurities. It has been demonstrated that a capacitive cell operating at radio frequency (10^5 Hz to 10^8 Hz) where the dielectric constants of air, ice, and liquid water are roughly in ratio 1:3:80 is a practical device for measuring the amount of liquid water in a given snow sample (Ambach and Denoth, 1975; Colbeck, 1978; Denoth et al., 1984). It is also known that the calibration of a snow capacitive cell is not trivial. One problem is that the shape and size of a snow cell should allow that either the sample can be cut from a snowpit wall or tested in situ, and should include sufficient snow volume to permit an independent measurement of liquid water. Such a cell is apt to have high "non-sample" capacitance owing to edge, ground and electrode effects (that is, high compared to cells normally used in materials testing). The latter contain the solid, liquid or gas in a shielded volume, with attention given to minimizing and correcting for the non-sample capacitance (Field, 1958). Another difficulty is that the measurements of snow properties used in the calibration (density, microstructure, snow liquid water) will have relatively high repeatability errors compared to similar measurements of more traditional materials.

In this paper we discuss some of the experimental and statistical problems in performing a calibration of a capacitive cell for the specific purpose of measuring snow liquid water. Surely, the geometry and frequency (one MHz) of our cell are not optimized, but we believe our methods, results and conclusions are relevant to other (better or worse) cell geometries and frequencies dedicated to that specific purpose.

EXPERIMENTAL METHODS

Our cell geometry (Fig. 1) consisted of four concentric cylinders imbedded in a PVC base defining a 1.6×10^6 mm^3 sample volume which could be either filled with natural or with artificially prepared snow. The cell was connected with alligator clips to the test fixture of a Hewlett–Packard 4271A impedance bridge, operating at fixed frequency (one MHz). We recorded capacitance C and loss tangent of the connected impedance, measured as a parallel combination of reactance X and conductance G. The loss tangent is often symbolized as tanδ, but in this paper we use XG.

With connections as in Fig. 1, the cell included three parallel capacitors having the sample space for dielectric, and three parallel capacitors having PVC for dielectric, formed where the bottom of the cyl-

0165-232X/88/$03.50 © 1988 Elsevier Science Publishers B.V.

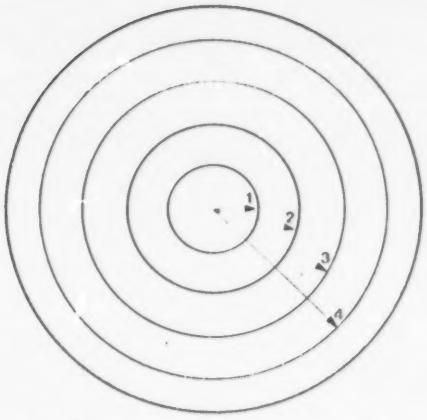

1. r = 25 mm
2. r = 50 mm
3. r = 75 mm
4. r = 100 mm

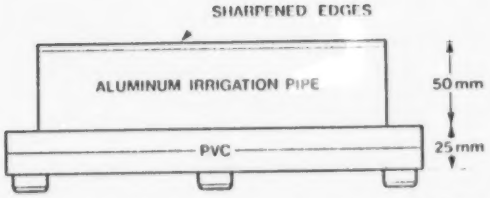

Fig. 1. Capacitive cell for measuring snow liquid water. Electrodes are connected 1 to 3, and 2 to 4, forming three parallel capacitors.

inders are set into the PVC base. The computed sum of these six capacitors is about 32 pF, whereas the measured capacitance C'_0 of the empty cell is 39 pF, repeatable to ±1 pF provided we replicated as closely as possible the position, connections and dryness of the cell during a C'_0 measurement. We associate the 7 pF difference with ground, edge and connection capacitance.

Natural snow samples were obtained from our subalpine study plot (Sunshine Village, Alberta, elev. 2300 m) during spring snowmelt when the snowpack thickness decreased from 1.2 m on 4 May 87 to virtually bare ground by June 87. Samples were cut in the cell from snowpit walls and carried about 25 m to a cold laboratory. Ambient temperature in the cold lab above our work space was maintained at 0°C±0.5°C except during early morning defrost. This was possible because we suspended the

TABLE I

Variation of capacitance and loss tangent XG with sample temperature T_s (retrozen snow, milled, sieved and compacted (476 kg/m^3))

T_s (°C)	C' (pF)	XG
−3.5	60.10	0.0156
−8.5	60.84	0.0586
−3.0	61.30	0.0887
−1.3	61.95	0.1183
−0.3	63.98	0.1375

thermistor which controlled refrigeration directly over the critical work area, and thereby sacrificed temperature control in the remainder of the lab. We monitored air, snow and water temperatures using factory calibrated thermometers (−10°C to +10°C, scale divisions 0.1°C).

Artificial prepared samples were used to study extremes of density and wetness. To prepare a "dry" sample (approx. 0% water) with temperature T_s in the range $-1 < T_s < 0$°C we filled the cell with snow, then placed it in a small freezer chest (−40°C) to drop T_s well below 0°C. We then gradually rewarmed the cell and monitored, C', XG and T_s. Table I gives typical data which show the accelerating rise of C' as T_s approaches 0°C. We attribute this effect to thickening of melt-like films on ice crystal surfaces.

To prepare samples with more liquid water than normally found in nature (> 20 g of water in 100 g sample) we added snowmelt from a 0°C icebath to wet samples. We did not systematically monitor or control the impurity content of samples and snowmelt, but did note a wide variation of specific conductance from about 10 μS/cm for "clean" melt to about 170 μS/cm for melt pooled at the bottom of the pack above frozen ground. By comparison, the conductivity of our deionized water is about 3 μS/cm. We observed some anomalously high XG readings that were probably due to impurity. In retrospect, we now consider it essential to monitor meltwater conductivity in future calibrations.

We prepared high density samples (> 500 kg/m^3) by compacting milled and sieved crust grains. The upper density limit, about 900 kg/m^3, was reached

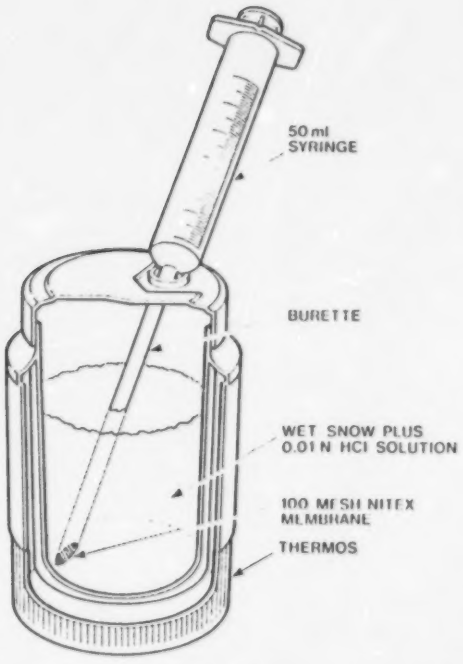

Fig. 2. Apparatus for acid dilution measurement of snow liquid water.

by refreezing slush and snowmelt in the cell; however it was difficult to trim samples to the defined cell volume owing to expansion during freezing.

Liquid water was measured independently using the acid dilution method (Davis et al., 1985) as follows. After measuring C' and XG we quickly transferred as much of the sample as possible from the cell into a thermos (vacuum flask type). Small amounts of the sample were invariably lost, but this was not an important source of scatter. Next, we quickly poured into the thermos a pre-weighed (about 500 g) solution of 0.01 N HCl, approximate conductance 4000 μS/cm, which had been stored overnight in an ice bath to guarantee 0°C (always checked within 0.1°C). The thermos was weighed, and then shaken for about 30 s. About 100 g of mixture were withdrawn through a 100 mesh nitex membrane into a burette and syringe as shown in Fig. 2. The ratio of sample conductance to reference conductance was determined at a later convenient time. Along with the solution and sample mass, this ratio was used to compute liquid water mass per

D (sample density, kg/m³)	W (liquid water mass/sample mass) 25%	50%	75%
250	8 Points C 46 pF XG 0 068	Missed	Missed	Missed
	175 Points C 79 pF XG 0 113	Missed	Missed	Missed
500	34 Points C 117 pF XG 0 158	17 Points C 227 pF XG 0 157	Missed	Missed
750	6 Points C 92 pF XG 0 206	5 Points C 499 pF XG 0 190	Missed	6 Points C 2057 pF XG 0 276

Fig. 3. Distribution of the 251 calibration points over the possible combinations of sample density and liquid water.

sample mass with an accuracy of ± 2 g water/100 g sample. Henceforth in this paper we symbolize mass of liquid water per sample mass as W, and use % in place of g/100 g. The sample density, density of ice and water are symbolized respectively as D, D_i and D_w.

One operator could complete a calibration point for a natural snow sample in 10 minutes or less. This included: cutting a sample from the snowpit, transporting it to the cold lab, weighing the sample to determine D, measuring C' and XG, transferring sample to thermos, checking temperature of HCl stock solution, adding solution, shaking thermos, weighing thermos, withdrawing mixture, checking cold lab temperature, lab clean-up (including cell and thermos), preparation for next sample, and recording all data.

STATISTICAL RESULTS

We measured 251 calibration points $\{C', XG, D, W\}$ which were distributed as in Fig. 3. The vast majority of points were for $W < 25\%$ and missed most of the extreme combinations. The difficulty is that if W exceeds about 25%, water percolates rapidly to the cell bottom and forms a layer. Sample capacitance increases as the water percolates downward, and C' cannot be measured as a steady value. We explain this instability later in the paper.

As evidenced in Fig. 3, C' increases with D and strongly with W. It also appears that XG increases

TABLE 2

Comparison of regression models for water W as a function of capacitance C and density D

Regression model	R^2
$W=\alpha+\beta D$	0.463
$W=\alpha+\beta C$	0.801
$W=\alpha+\beta C+\gamma D$	0.893
$W=\alpha+\beta C+\gamma D+\delta D^2$	0.903
$W=\alpha+\beta C+\gamma D+\delta C^2$	0.931
$W=\alpha+\beta C+\gamma D+\delta CD$	0.968
$W=\alpha+\beta C+\gamma D+\delta C^2+\delta D^2+\zeta CD$	0.970

with D and somewhat with W. Perhaps the W-variation is obscured by lack of impurity control, as already noted. To test the relative importance of C, D, and XG as statistical predictors of W, we performed the linear multiple regression

$$W=\alpha+\beta C+\gamma D+\delta XG \tag{1}$$

on the 251 calibration points (Fig. 3) plus an additional 200 empty cell reference points. The goodness-of-fit R^2 was found to be 0.895, and the correlation matrix $[r_{ij}]$ to be

$$[r_{ij}]=\begin{pmatrix} \ldots & W & C & D & XG \\ W & 1.00 & 0.89 & 0.68 & 0.53 \\ C & 0.89 & 1.00 & 0.46 & 0.35 \\ D & 0.68 & 0.46 & 1.00 & 0.69 \\ XG & 0.53 & 0.35 & 0.69 & 1.00 \end{pmatrix} \tag{2}$$

To test the least significant predictor XG we considered these alternative models that omit XG

$$W=\alpha+\beta C+\gamma D \tag{3}$$

and

$$W=\alpha+\beta C+\gamma D+\delta CD \tag{4}$$

The respective R^2 for eqns. (3) and (4) are 0.893 and 0.986 which suggest there is no advantage to using XG as a predictor in a statistical calibration based on our data set. This may not be the case in studies that better control impurities and microstructure, that sweep frequencies, or use physical models that depend on complex impedance. Henceforth we base our discussion on the restricted data $\{C,D,W\}$.

Table 2 compares statistical models of $W(C,D)$ through second order and involving no more than six regression coefficients. These models have virtually no physical meaning and are unstable in the signs and magnitudes of the coefficients. Further improvement depends on supplementing the statistical approach with physical concepts.

LINEAR CALIBRATION MODEL

First, it is instructive to consider Fig. 4, which shows capacitance of the cell as it is filled to various levels with 0°C snowmelt, i.e. C as a function of D for the extreme case $W=100\%$. Despite scatter due to impurities, ice nucleation at 0°C, and poor repeatability of the "full to the brim" level $D/D_w=1$, C is nevertheless very close to a linear function of D with $R^2=0.997$. The reason for linearity is that an incremental increase in water level is physically equivalent to adding capacitance incrementally, with negligible depolarization from another phase.

Next, consider Fig. 5 which represents dry snow data ($W=0\%$ and $-1\leq T_c<0$°C). Here scatter is due to the relatively large fluctuation of C versus T_c near 0°C as illustrated in Table 1. Also, there is repeatability error for the "full to the brim" with ice (D/D_w about 0.9). However, the way we packed lower density snow into the cell did not change C by more than 0.5 pF. Even if we poked about 100 small holes in the sample, C was less influenced by that mechanical disturbance than by small temperature fluctuation. The departure from linearity in Fig. 5 is explained by envisioning the dry snow microstructure to be a network of small ice capacitors. At high density, D/D_w approaching 0.9, these micro-capacitors tend to add with little depolarization, but as density lowers there are fewer micro-capacitors and an increasing depolarization due to the presence of the pore space. This effect does not produce strong nonlinearity ($R^2=0.984$) since the one MHz dielectric constants of air (about one) and ice (about three) are not far apart, and depolarization is weak.

Let us first try a linear model where snow sample capacitance C_s is assumed to be a combination of the individual phases. Thus, following Gerdel (1954), we first try

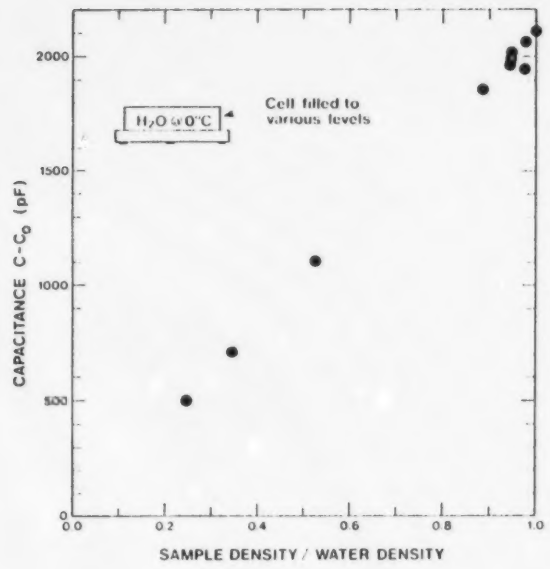

Fig. 4. Linear increase of capacitance with increassing sample density for the special case $W = 100\%$, simulated by increasing water level in the cell.

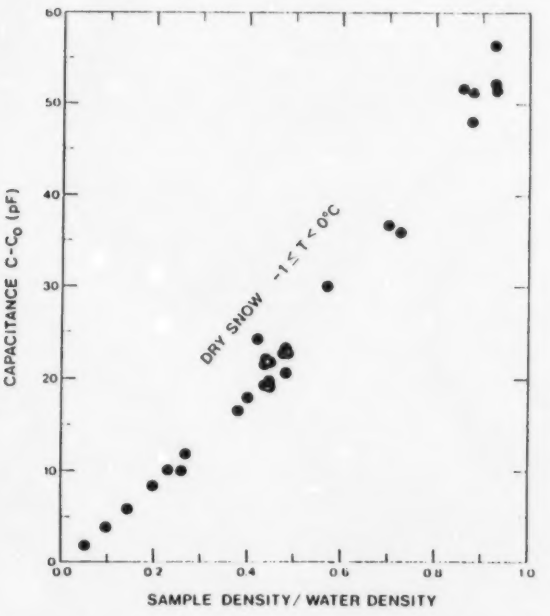

Fig. 5. Capacitance versus sample density for dry snow $W \approx 0\%$.

$$C_s = k_a V_a + k_i V_i + k_w V_w \tag{5}$$

where V_a, V_i and V_w are the relative volumes of the air, ice and water in the sample such that $V_a + V_i + V_w = 1$, and where k_a, k_i and k_w are assumed to be constants that are derivable from cell geometry and the respective dielectric constants. The transformation from relative volumes to the measured parameters D and W is

$$\begin{bmatrix} 1 \\ D \\ DW \end{bmatrix} = \begin{bmatrix} 1 & 1 & 1 \\ 0 & D_i & D_w \\ 0 & 0 & D_w \end{bmatrix} \begin{bmatrix} V_a \\ V_i \\ V_w \end{bmatrix} \tag{6}$$

Independent of assumptions implicit in eqn. (5), we further assume that the measured C is the parallel combination of sample capacitance C_s and non-sample capacitance C_c, as discussed earlier. Thus $C = C_s + C_c$. The measured capacitance of the empty cell is

$$C_0 = k_a (V_a + V_i + V_w) + C_c \tag{7}$$

and therefore

$$C = C_0 + (k_i - k_a) V_i + (k_w - k_a) V_w \tag{8}$$

Using multilinear regression on our 251 points $\{C, D, W\}$ plus 200 additional $\{39, 0, 0\}$ empty cell points introduced to force C_0 to approach 39 pF, we find

$$C = 38.7 - 109 V_i + 194 V_w \tag{9}$$

Although this is a statistical fit ($R^2 = 0.96$), it is a poor physical model which fails completely to fit dry snow data because of the negative V_i term, despite the small positive correlation between C and V_i shown in the correlation matrix for (9)

$$[r_{ij}] = \begin{pmatrix} \cdots & C & V_i & V_w \\ C & 1.00 & 0.02 & 0.97 \\ V_i & 0.02 & 1.00 & 0.14 \\ V_w & 0.97 & 0.14 & 1.00 \end{pmatrix} \tag{10}$$

The difficulty with a linear model is that because V_w is completely dominant, the plane of fit is positioned such that increasing V_w decreases the effect of V_w.

NONLINEAR CALIBRATION MODEL

It therefore appears necessary to replace eqn. (5) with a nonlinear equation, but what is the physical origin of any strong nonlinearity? First, it should be understood that the linearity in Fig. 4 is deceiving, for if the water in the cell could somehow be dispersed as a network, in contrast to layers, $C(D,100\%)$ would be strongly curved, much more so than Fig. 5 because the dielectric constant of water is about 80 times that of air at one Mhz, and thus the depolarization is much stronger than in the dry snow case. This explains the rising C that is observed when water is settling to form a layer at the bottom of the cell, for during this process there is a transformation from a dispersed to a layered mixture, where depolarization is significantly lower.

A nonlinear model can be based, therefore, on the assumption that increasing V_a and/or V_w not only implies a reduction of $k_i V_i$ since there is less ice, but also a reduction due to increased depolarization of the ice microstructure by the other phases; likewise, increasing V_w and/or V_i causes the similar reduction in $k_w V_w$. This assumption means that eqn. (5) should be replaced by an expression that accounts for phase cross-effects

$$C_c = k_a V_a + k_i(1 - k_{ia} V_a - k_{iw} V_w) V_i + k_w(1 - k_{wa} V_a - k_{wi} V_i) V_w \quad (11)$$

where the double subscripted constants depend on microstructure. Assuming eqn. (7) as before, terms are combined in eqn. (11) to form the multilinear regression equation

$$C = \alpha + \beta V_i + \gamma V_w - \delta V_a V_i - \epsilon V_i V_w - \zeta V_a V_w \quad (12)$$

which we tested as before using 251 points $\{C,D,W\}$ plus 200 points $\{39,0,0\}$ to force $\alpha = C_0 = 39$ pF, and obtained with coefficients rounded to the nearest integer

$$C = 40 + 48 V_i + 2166 V_w - 231 V_a V_i - 1060 V_i V_w - 2275 V_a V_w \quad (R^2 = 0.9977) \quad (13)$$

Note all coefficients (including β) appear with the sign and magnitude expected on physical grounds.

Table 3 summarizes the mean algebraic error A and the mean absolute error $|A|$ computed using

$$A = \frac{1}{N} \sum^{N} (W_i^{(R)} - W_i) \quad (14)$$

$$|A| = \frac{1}{N} \sum^{N} |W_i^{(R)} - W_i| \quad (15)$$

where $W_i^{(R)}$ is the value predicted using eqn. (13) with substitution of measured C_i and D_i which correspond to measured W_i. The 200 empty cell points are not included in the computation of A and $|A|$. Note in Table 3 that the model performs best over the range of natural wetness $W \leq 20\%$, and diverges with increasing range. Perhaps some of the divergence could be removed if data for completion of Fig. 3 were included along with additional reference points at $W = 0\%$ and 100% with $D/D_w \approx 1$.

TABLE 3

Algebraic A and absolute $|A|$ errors using regression eqn. (13)

Max W (%)	N	A (%)	$\lvert A \rvert$ (%)
10	124	0.36	1.46
20	212	−0.84	2.02
30	231	−1.27	2.36
40	242	−1.66	2.70
50	245	−1.79	2.81
100	251	−2.62	3.62

As a further test, we performed the six coefficient regression of the second order statistical model

$$C = \alpha + \beta D + \gamma W + \delta D^2 + \epsilon W^2 + \zeta W D \quad (16)$$

using our 251 points $\{C,D,W\}$ plus 200 points $\{39,0,0\}$ and obtained $R^2 = 09968$. However, computations using eqns. (14) and (15) were impossible because $W_i^{(R)}$ was often a complex number on substitution of C_i and D_i into eqn. (16). Three, four and five coefficient models obtained by eliminating terms from eqn. (16) produced, in addition to lower R^2, a variety of sign and magnitude combinations which suggest that eqn. (16) is unstable, at least for our data set.

CONCLUSIONS

Calibration of a capacitive cell for measuring snow water in field and laboratory involves a statis-

tical fit of measurements (capacitance C', density D, and water W') to nonlinear functions of $W'(C',D)$ or $C'(D,W')$ where the latter must provide real (non-complex) W' for measured C' and D. There is probably no unique or optimum function, except that one seeks physically meaningful functions with minimum adjustable parameters giving high goodness-of-fit (i.e. high R^2). We found that a function based on cross effects between phases gave $R^2=0.998$, and suspect that the fit could be improved if we had more and better data at the reference extremes, better control of meltwater impurities, better control of microstructure, and perhaps most important, improvement in cell design and frequency choice. In the present study, dielectric loss ($\tan\delta=X/G$) was found to be a relatively poor predictor of W', but this may not be the case in an improved study.

REFERENCES

Ambach, W. and Denoth, A. (1975). On the dielectric constant of wet snow. Snow Mechanics Symp., Int. Assoc. Hydrol. Sci., Publ., No. 114: 136–141.

Colbeck, S.C. (1978). The difficulties of measuring the water saturation and porosity of snow. J. Glaciology, 20(82): 189–201.

Davis, R.E., Dozier, J., Lachapelle, E.R. and Perla, R. (1985). Field and laboratory measurements of snow liquid water by dilution. Water Resour. Res., 21(9): 1415–1420.

Denoth, A., Foglar, A., Weiland, P., Mätzler, C., Aebischer, H., Tiuri, M. and Sihvola, A. (1984). A comparative study of instruments for measuring the liquid water content of snow. J. Appl. Physics, 56(7): 2154–2159.

Field, R.F. (1958). Dielectric measuring techniques. in: A.R. VonHippel (Ed.), Dielectric Materials and Applications. Technology Press of M.I.T. and John Wiley & Sons, Chapter II, AI: 47–62.

Gerdel, R.W. (1954). The transmission of water through snow. Trans. Amer. Geophys. Union, 35(3): 475–485.